第８回地震時保有耐力法に基づく橋梁等構造の
耐震設計に関するシンポジウム講演論文集（2005 年 2 月）

ENHANCEMENT OF SHEAR STRENGTH AND DUCTILITY OF RC PIERS BY CONTROLLING BOND OF REINFORCING BARS

Govinda Raj Pandey[1], Takeshi Maki[2], Hiroshi Mutsuyoshi[3], Ryosuke Tanino[4], Enkhtur Shoordor[5]

[1]JSPS Postdoctoral Fellow, Saitama University （〒338-8570 Shimo-Okubo, Sakura-ku, Saitama-shi, Saitama)
[2]Research Associate, Saitama University （〒338-8570 Shimo-Okubo, Sakura-ku, Saitama-shi, Saitama)
[3]Professor, Saitama University （〒338-8570 Shimo-Okubo, Sakura-ku, Saitama-shi, Saitama)
[4]Graduate Student, Saitama University （〒338-8570 Shimo-Okubo, Sakura-ku, Saitama-shi, Saitama)
[5]Graduate Student, Saitama University （〒338-8570 Shimo-Okubo, Sakura-ku, Saitama-shi, Saitama)

1. Introduction

Recent severe earthquakes, such as Hyogoken- Nanbu Earthquake in 1995, have given numerous examples of catastrophic shear failure of RC bridge piers leading to their fatal collapse [1]. Following the earthquake, design earthquake loads in Japanese design codes have been drastically increased and performance based design concept is introduced so that the structure possesses required seismic performance after an earthquake [2]. To satisfy the seismic performance required by new design codes, an enormous amount of shear reinforcements have to be provided in RC bridge piers. A large quantity of reinforcement however makes its arrangement complicated and congested creating constructability problems [3]. It is therefore important to look for some alternative methods to improve shear capacity without relying heavily on shear reinforcement alone.

Altering the bond conditions between the longitudinal bars and the concrete has a major effect on the behavior of RC members. Kani showed that beams with round bars have a higher shear capacity than beams with deformed bars [4]. He explained that the increase in the shear capacity is due to the presence of weaker bond in the round bars.

A large number of experimental and analytical studies carried out on columns with bond controlled reinforcing bars showed that the technique of unbonding reinforcing bars is very effective in enhancing seismic performance of RC piers [5-7]. The change in the internal mechanism of RC piers with the bond condition, however, is far from being well understood.

The main objective of this study is to investigate the behavior of RC columns with bond controlled reinforcing bars. The aim is also to utilize analytical tools in order to clarify the change in the internal mechanism which is responsible for the abrupt change in the behavior of piers with unbonded longitudinal bars compared to those with ordinary deformed bars.

2. Experimental Program

In order to investigate the influence of unbonding reinforcement on shear strength and ductility of RC piers, four specimens were tested under reversed cyclic loading.

(1) Specimen Details

Specimens were divided into two series depending on shear-span-to-depth (a/d) ratio. **Fig-1** shows the geometry and reinforcement details of the test specimen. Every

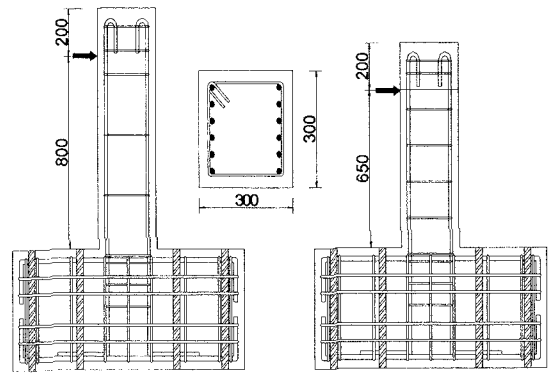

Fig-1 Details of column specimens

specimen consisted of column part cast monolithically with footing part. Cross-section of all the specimens were 300 x 300 mm while the height of the columns were 1000 mm and 850 mm for specimens of A-Series and B-Series respectively. Shear capacity of concrete, was evaluated by using Okamura-Higai as shown in Equation **(1)**.

$$V_c = 0.2 f_c'^{1/3} (100 p_w)^{1/3} (\tfrac{1000}{d})^{1/4} (0.75 + 1.4 \tfrac{d}{a}) b_w d \quad (1)$$

where,
f_c' = compressive strength of concrete
p_w = ratio of tensile longitudinal steel area to area of web concrete
d = effective depth
a = shear span
b_w = web width of member

Okamura-Higai equation was used because it incorporates the effect of a/d ratio. Design shear strength to flexural strength ratio of 0.8 was employed in the experiment. Identical longitudinal reinforcement details with 12 bars of 16 mm in diameter were incorporated in all the test specimens. Deformed bars with the diameter of 6 mm were used as lateral reinforcement. **Table-1** shows the details of the test specimens.

Table-1 Details of the column specimen

Sp. No.	a/d	Bond condition	Longitud -inal bars A_s	Lateral ties Size and spacing(mm)
A-1	3.0	Deformed bars	12-D16	D6@250
A-2		Unbonded bars	12-D16	D6@250
B-1	2.5	Deformed bars	12-D16	D6@150
B-2		Unbonded bars	12-D16	D6@150

(2) Material Properties

Ready-mix, normal weight concrete with an average slump of 150 mm was used. Compressive strength test on concrete cylinders and tensile strength test on steel samples were performed to determine the actual material properties of the concrete and reinforcing steel. **Table-2** presents the compressive strength of concrete on the day of cyclic loading test and the yield strength of the various types of steel used in the specimen.

Table-2 Material properties of the column specimen

Sp. No.	Concrete f_c', MPa	Longitudinal bars f_y, MPa	Lateral ties f_{wy}, MPa
A-1	32.54	380.18	396.60
A-2	33.69	380.18	396.60
B-1	28.76	380.18	396.60
B-2	30.47	380.18	396.60

(3) Method of Controlling Bond

Fig-2 shows the methods used in bond control. In the specimens with perfect bond normal deformed bars were used as longitudinal reinforcement.

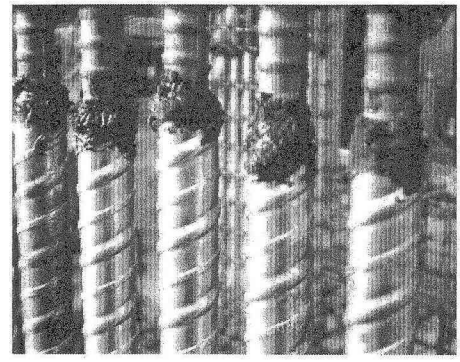

(b) Perfect Unbond
Fig-2 Method of controlling bond

Complete unbonding of longitudinal bar was achieved by the use of spiral sheath. Before casting the specimen, the desired length of longitudinal bar was inserted into the sheath. The location of the sheath was properly fixed and the both the end of the sheath were made water tight by applying silicon gel.

(4) Experimental Setup and Instrumentation

Fig-3 shows the loading setup. The specimen was fixed on the floor with prestressing rods. Reversed cyclic lateral load was applied at the designated loading point of the column by using an actuator. A constant axial load of 90 kN was applied throughout the experiment in order to maintain the compressive stress of 1 MPa. Axial loading jack was designed to move freely with applied lateral displacement.

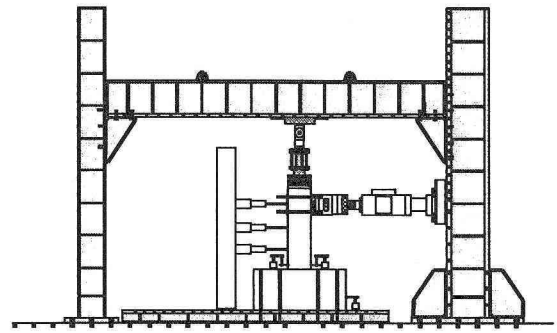

Fig-3 Experimental setup

Horizontal displacements at three different locations in the column, crack width at the column-footing joint and possible displacement and rotation of the specimen were

measured by displacement transducers. Strains in several locations of both longitudinal bars and lateral reinforcement were measured by using strain gages which were already fixed at the desired location before placing concrete.

(5) Reverse Cyclic Loading Test

All the specimens were subjected to reverse cyclic quasistatic loading with the loading sequence shown in **Fig-4**. Each displacement amplitude was prolonged for a set of three cycles. The first set of cycles was essentially within the elastic range and with the increase in the number of cycles the specimen entered to the inelastic range. In the first set of cycles, the specimen was subjected to the displacement amplitude of H/200, where H is the height of the lateral loading point from the column base. Displacement amplitude was then increased with an increment of H/200 until the specimen failed. The specimen was considered to have failed when the load carrying capacity was reduced to the 80% of its maximum recorded load.

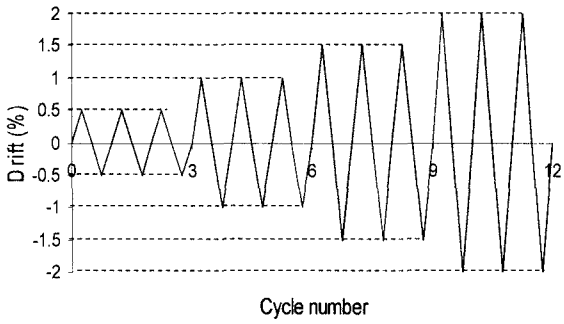

Fig-4 Loading sequence

3. Results and Discussion

(1) Load-Displacement Curve

Load-displacement curves obtained from the experiment for both A-Series and B-Series are shown in **Fig-5**. Specimen A-1 failed in shear before yielding of the longitudinal bars. Specimen A-2 with unbonded longitudinal bars completely avoided shear failure and eventually failed due to crushing and spalling of concrete followed by yielding of longitudinal bars. Unlike A-1, Specimen B-1 failed in shear after the longitudinal bars yielded. With the change in the bond condition, similar to A-Series, B-Series also showed improvement in ductility and complete change in the failure mechanism from shear to flexure.

Pinching effect was clearly visible in the load displacement curves. This effect was attributed to the closure of diagonal shear crack with the load reversal in the case of Specimens A-1 and B-1. On the other hand, pinching in unbonded specimens was due to the closure of large flexural crack at column-footing joint.

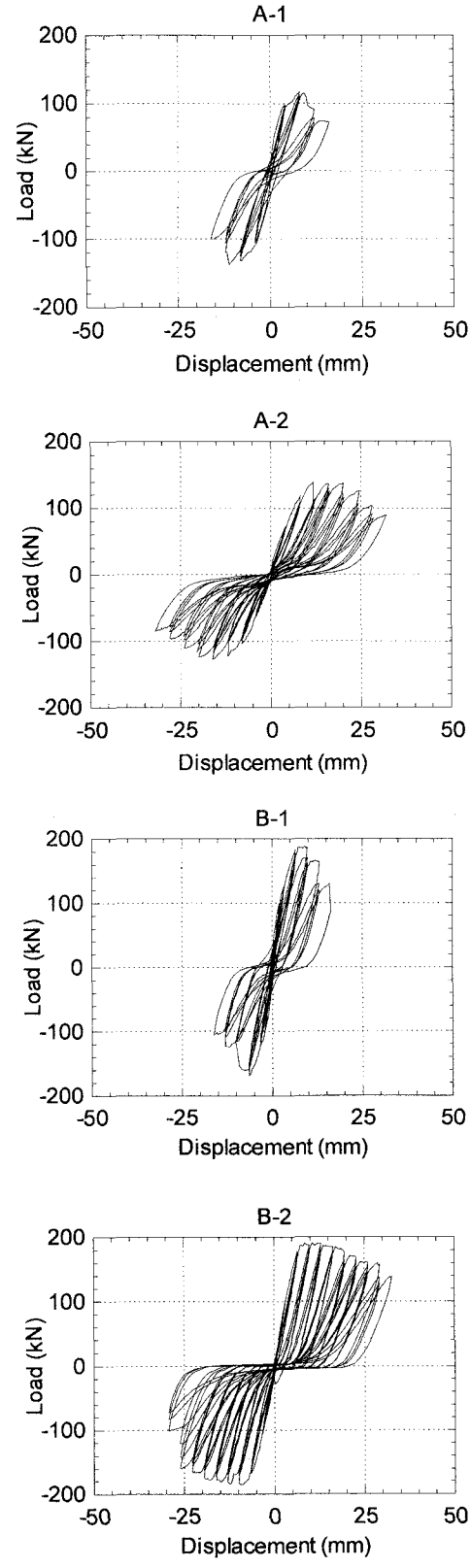

Fig- 5 Load displacement curves of all tested specimens

(2) Failure Pattern

Fig-6 shows the crack pattern of all the specimens at failure. In the case of specimens A-1 and B-1, flexural cracks occurred at the several locations on the specimen right from the first cycle. As the number of cycles increased, the crack furthered and then developed to diagonal shear crack. The final failure took place with the wide opening of diagonal crack resulted from the yielding of shear reinforcement. Load-displacement curve clearly shows a typical shear behavior.

In case of specimens A-2 and B-2, the crack started from the column-footing joint first. With further loading the crack at the bottom increased and propagated upwards. No single crack was formed at the sides of the specimen. The final failure was due to the crushing of concrete followed by yielding of the longitudinal bars.

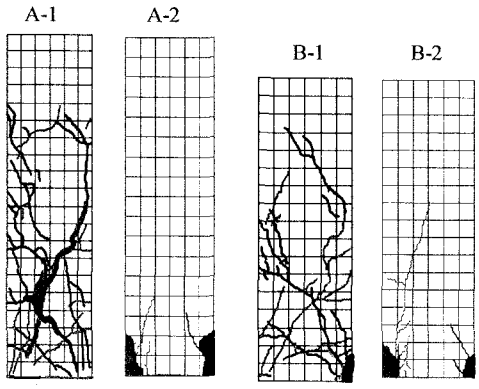

Fig-6 Crack pattern of specimen at failure

4. Finite Element Analysis

Three-dimensional nonlinear finite element analysis was performed to replicate the quasistatic reversed cyclic loading test.

(1) Finite Element Model

A twenty node isoparametric solid element with eight point gauss integration scheme is used to model concrete. Reinforcing bar is modeled as one dimensional three node beam element with six degrees of freedom per node including three translation and three rotation degrees of freedom. Bond between steel and concrete is modeled by one dimensional six node joint element. By varying shear stiffness of the joint element, various bond conditions from the perfect bond as that of ordinary RC column to the perfect unbond can be achieved. In RC columns, footing region is modeled as solid elastic concrete elements with the boundary nodes restrained in all three directions.

(2) Material model

The nonlinear material model for reinforced concrete is composed of several models to characterize the behavior of concrete and reinforcing bars. The nonlinearity in the reinforced concrete is due to the cracking of concrete, yielding of longitudinal bars and the bond interaction between steel and concrete. To be able to use in finite element analysis, space-averaged stress-strain relationship is formulated for plain element in which both cracks and longitudinal bars are smeared over the whole element. The total stress is then evaluated as the sum of the averaged stresses of cracked concrete and the reinforcement at equilibrium [8]. Models for concrete can be broadly divided into the one before and after cracking which is separated by a cracking criterion.

In order to model the nonlinearity of concrete before cracking, elasto-plastic fracture (EPF) model is used. In the model, the permanent deformation and loss of elastic strain energy absorption of uncracked concrete is idealized as the combination of plasticity and continuum fracture [9]. Cracking in concrete changes its behavior and it becomes anisotropic in the crack direction. For the cracked concrete, the orthogonal four-way fixed crack model is used to obtain three constitutive laws of cracked concrete including normal stress transfer parallel and normal to the crack axis and shear stress transfer along the crack interface which are termed as compression, tension and shear transfer model respectively.

Compression stress parallel to the crack is modeled similar to the EPF model. In the model the compressive normal stress parallel to the crack direction is assumed to be uniaxial as the stress can release in the orthogonal direction [10]. The ability of cracked concrete to carry tensile stress are taken into account by incorporating tension stiffening and softening models. Shear transfer models are used to model shear stress transfer along the crack surface. Reinforcing bar is modeled based on the properties of bare bar and the effect of bond between steel and concrete.

(3) Results and discussion

Cyclic analysis on RC bridge piers is conducted to characterize the global hysteretic behavior including stiffness, strength, ductility, energy absorption capacity and residual deformation. The load displacement curves determined at the loading point were measured in the experiment and calculated in the simulation. The comparisons of these curves are shown in **Fig-7**.

Agreeing well with the experimental results, both the specimens with perfect bond failed in shear. Specimens B-1 failed in shear soon after the yielding of longitudinal bar. In series A, however, specimen A-1 failed in shear prior to flexural yielding. The analytical results show that the developed finite element analysis can accurately predict the ultimate load and hysteretic behavior.

In all the specimens with the deformed bars unbonded with surrounding concrete, a drastic improvement in the seismic performance was observed. Since a complete change in the mechanism of unbonded specimens was

observed, the use of finite element method was attempted to investigate the alteration. Analytical results of the unbonded specimens of both the series, A-2 and B-2 have shown that the ultimate load capacity and hysteretic behavior could be very well predicted by the proposed finite element analysis. Analytical results, however, underestimate the ductility.

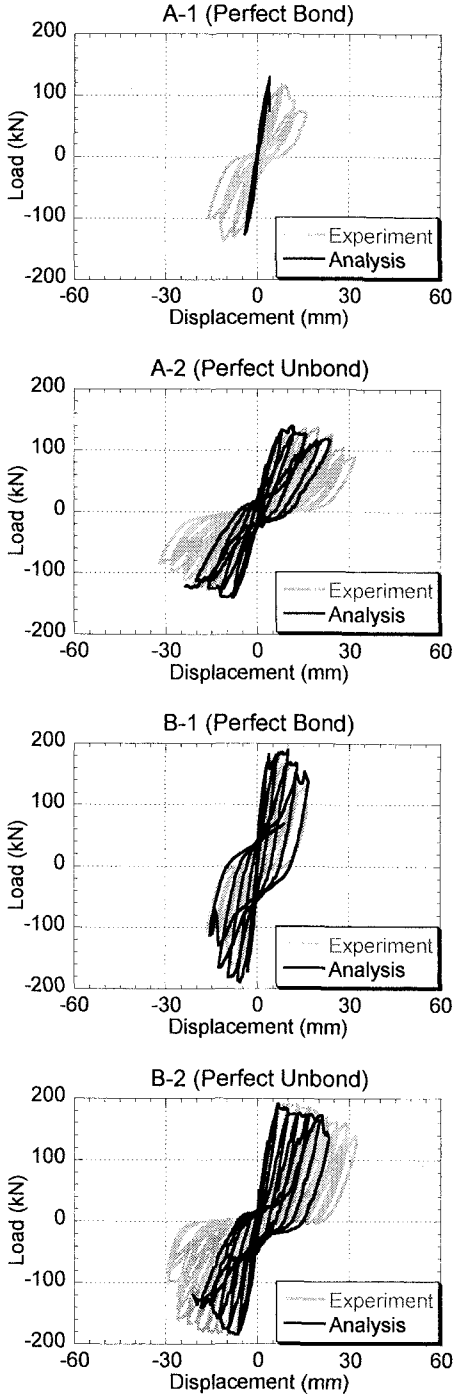

Fig-7 Comparison of experimental and analytical hysteretic behavior

(4) Stress Distribution

The stress flow diagram obtained from the analysis for specimens B-1 and B-2 both before and after the initiation of the first flexural crack is shown in Figure 8. Specimen B-1 showed a curvilinear flow of principal compressive stress both before and after the occurrence of flexural crack. This stable behavior is attributed to the stress transfer from steel to concrete due to the presence of bond.

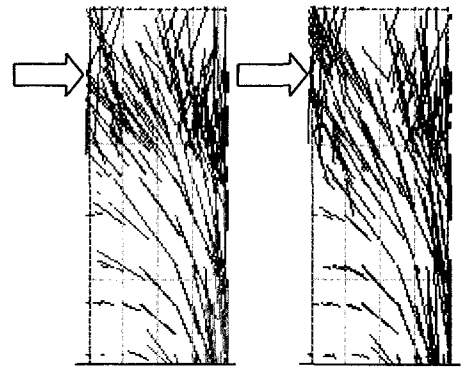

B-1 B-2

(a) Before the first flexural crack

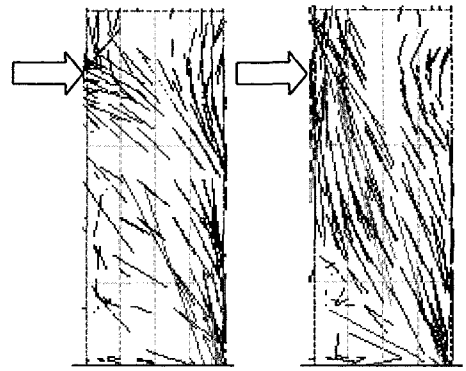

B-1 B-2

(b) At the lateral load of 100kN

Fig-8 Stress flow diagram

Before the first flexural cracking, stress flow pattern of Specimen B-2 is similar to the one of B-1. Before cracking, the tensile stress developed in the concrete is responsible for this type of stress flow. A clear change in the behavior of Specimen B-2 is observed after the appearance of the first flexural crack. The stress in the column is transferred from loading point to the support by straight diagonal thrust lines resembling the behavior of tied arch. Since the pier is in the state of diagonal compression, the stress condition of concrete is favorable in preventing shear failure.

5. Conclusion

Reversed cyclic loading test and three dimensional nonlinear finite element analysis was carried out on four RC columns with various bond conditions of longitudinal reinforcement. Based on this study following conclusions can be drawn:

1. Unbonding of longitudinal bar can completely change failure mode at the ultimate state from shear to flexure and it remarkably increases the ductility.
2. Described finite element model is able to anticipate the behavior of both bonded and unbonded RC piers with reasonably accurate estimation of maximum load, failure mode and ductility.
3. An abrupt change in the behavior of unbonded pier occurs after the initiation of the first flexural crack which is an onset to new mechanism.
4. Behavior of unbonded pier matches to the one of tied arch with a straight thrust line joining support and loading point. Due to this stress transfer mechanism, unbonded piers do not fail in shear and shows an enhanced ductility.
5. Small amount of hysteretic energy absorption is evident in the unbonded piers which are basically due to the opening of wide flexural crack at the column-footing joint.

References

1) Okamura, H., "Japanese Seismic Design Codes Prior to Hyogoken-Nanbu Earthquake," *Cement and Concrete Composites*, Vol. 19, 1997, pp. 185-192.
2) Standard Specification for Design and Construction of Concrete Structures (Seismic Design), Japan Society of Civil Engineers, 2002. (in Japanese)
3) Naito, C. J.; Moehle, J. P.; and Mosalam, K. M., "Evaluation of Bridge Beam-Column Joints under Simulated Seismic Loading," *ACI Structural Journal*, V. 99, No. 1, January-February 2002, pp. 62-71.
4) Kani, G. N. J., "The Riddle of Shear Failure and its Solution," *ACI Journal*, Vol. 61, No. 4, April 1964, pp. 441-467.
5) Pandey, G. R., Mutsuyoshi, H., Sugita, K. and Uchibori, H., "Mitigation of Seismic Damage of RC Structures by Controlling Bond of Reinforcement", Proc. of Japan Concrete Institute, Vol. 25, 2003, pp. 1441-1446.
6) Pandey, G. R., Mutsuyoshi, H., "Enhancement of Seismic Performance of RC Structures by Controlling Bond of Reinforcement", Proc. of 7th Symposium on Ductility Design Method of Bridges, JSCE, 2004, pp. 39-46
7) Pandey, G. R., Mutsuyoshi, H., "Seismic Damage Mitigation of Reinforced Concrete Bridge Piers by Unbonding Longitudinal Reinforcement", Proc. of 13th World Conference on Earthquake Engineering, 2004.
8) Okamura, H. and Maekawa, K., "Nonlinear Analysis and Constitutive Models of Reinforced Concrete," Gihodo-Shuppan Co. Tokyo, 1991.
9) Maekawa, K. and Okamura, H., "The Deformation Behavior and Constitutive Equation of Concrete using Elasto-Plastic and Fracture Model," J. Faculty Eng., University of Tokyo (B), Vol. 37, No. 2, 1983, pp. 253-328.
10) Collins, M. P. and Vecchio, F., "Response of Reinforced Concrete in-plane Shear and Normal Stress," University of Toronto, 1982.